EQUILIBRIUM MODELING OF CLINOPTILOLITE-ANALCIME EQUILIBRIA AT YUCCA MOUNTAIN, NEVADA, USA

Steve J. Chipera and David L. Bish

Earth and Enviromental Sciences, Los Alamos National Laboratory,
Mail Stop D469, Los Alamos, New Mexico 87545

Abstract—Yucca Mountain, Nevada, is being investigated to determine its suitability to host a potential high-level radioactive waste respository. An important reason for its choice as a potential repository site was the presence of thick zeolite-rich horizons in the altered volcanic tuffs that compose the mountain. Clinoptilolite is the most abundant zeolite at Yucca Mountain and may be important in radionuclide retardation and in determining hydrologic properties. Therefore, it is necessary to understand the geochemical conditions affecting its long-term stability. For example, it has been suggested that long-term, repository-induced heating of the rocks at Yucca Mountain may lead to the transformation of clinoptilolite to analcime, thereby significantly affecting the hydrologic properties and retardation capabilities of the rock.

Thermodynamic modeling of clinoptilolite-analcime equilibria was conducted with the program Ge0-Calc PTA-SYSTEM using estimated thermodynamic data for measured chemical compositions of clinoptilolite and analcime at Yucca Mountain. $\log[(aK^+)^2/aCa^{2+}]$ versus $\log[(aNa^+)^2/aCa^{2+}]$ diagrams were calculated to model the conditions under which clinoptilolite may transform to analcime. Temperature, relative cation abundances and silica activity are all important factors in determining clinoptilolite-analcime equilibria. Increased Na^+ concentrations in either clinoptilolite or the fluid phase, increased clinoptilolite K^+ concentration, increased temperature and decreased aqueous silica activity all stabilize analcime relative to clinoptilolite, assuming present-day Yucca Mountain water compositions. However, increased Ca^{2+} concentrations in either clinoptilolite or the fluid phase, increased aqueous K^+ concentration and increased Al:Si ratios in clinoptilolite (heulandite) all stabilize clinoptilolite with respect to analcime.

Assuming well J-13 water as the analog chemistry for Yucca Mountain water, clinoptilolite should remain stable with respect to analcime if temperatures in the clinoptilolite-bearing horizons do not significantly exceed 100 °C. Even if temperatures rise significantly (for example, to 150 °C), not all clinoptilolite should alter to analcime. Perhaps more importantly, thermodynamic modeling suggests that some Yucca Mountain clinoptilolites, particularly those rich in Ca and Al, will remain stable at elevated temperatures, even with an aqueous silica activity at quartz saturation.

Key Words—Analcime, Clinoptilolite, Modeling, Stability, Thermodynamic, Zeolite.

INTRODUCTION

Yucca Mountain, in southern Nevada, is being investigated to determine its suitability to host the first high-level radioactive waste repository in the United States (Figure 1). The presence of thick zeolite-rich horizons formed by alteration of the volcanic ash-flow tuffs (12–15 My) that make up the mountain is one of the primary reasons that Yucca Mountain was chosen as a potential repository site. The proposed repository horizon is above the static water level in the welded, devitrified Topopah Spring Tuff, which consists primarily of alkali feldspar, quartz and cristobalite.

The zeolitic alteration at Yucca Mountain was described by Smyth (1982) and Broxton et al. (1987) as consisting of 4 characteristic diagenetic zones based on mineralogy (as defined by Iijima 1975, 1978). Zone I is the shallowest and is characterized by vitric tuffs containing unaltered volcanic glass and minor smectite, opal-CT, heulandite and Ca-rich clinoptilolite. Zone II is characterized by the complete replacement of volcanic glass by clinoptilolite ± mordenite and by lesser amounts of opal-CT, K-feldspar, quartz and

smectite. Zone III consists of analcime, K-feldspar, quartz and minor calcite and smectite. Zone IV is characterized by albite, K-feldspar, quartz and minor calcite and smectite. Depending upon exact placement in the repository block, the repository horizon, at ~320 m depth in devitrified tuff, is directly underlain by either Zone I or Zone II assemblages. Figure 2 is a schematic diagram showing the depths of the repository horizon, the first major zeolitic horizon (diagenetic Zone II—zeol), the static water level (SWL), the first occurrence of analcime (diagenetic Zone III—analc-in) and the approximate depth where the thick sequences of clinoptilolite terminate (cpt-out) for drill holes in the Yucca Mountain vicinity. Depths in feet have been included on Figure 2 to correspond with the labels of the samples analyzed for chemistry (Broxton et al. 1986) and mineralogy (Bish and Chipera 1989).

It is perhaps universally agreed that emplacement of high-level radioactive waste in the rocks at Yucca Mountain will give rise to long-term elevation of temperature in the rocks surrounding the repository horizon. Given present-day rock properties, the exact na-
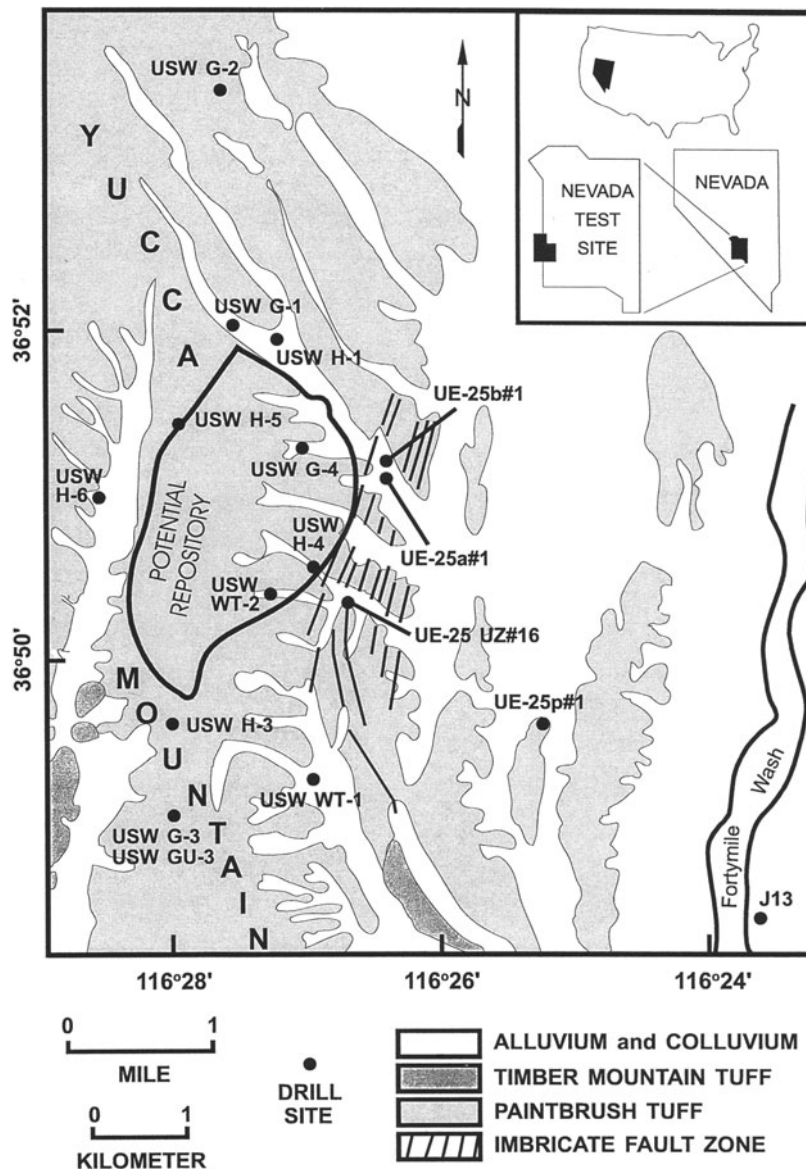
226

Figure 1.   Map of Yucca Mountain, Nevada, showing the locations of drill holes discussed in the text.

ture of the temperature distribution and the time-temperature history depend primarily on the details of the waste package distribution (such as geometry and packing density) and how much radioactive waste is emplaced within a given area. This latter parameter is usually stated in terms of areal mass loading (AML) in units of metric tons of U/acre (MTU/acre) or areal power density (APD) in units of kW/acre. The age of the spent fuel is required to translate AML to APD, as the power density decreases with time. The baseline APD used in the Yucca Mountain Site Characterization Plan is 57 kW/acre (an AML of 55.3 MTU/acre for 22.5-year-old fuel). However, more recent models of the thermal behavior of a repository at Yucca

Mountain have considered the benefits of higher loadings, up to an AML of 110.5 MTU/acre (Buscheck et al. 1994). These benefits include formation of a large dry-out zone around the repository horizon, with the possibility of associated condensate drainage, for times extending well beyond 1000 y. These recent models suggest that liquid saturation in much of the repository horizon will remain below initial values (>68%, Buscheck et al. 1994) for at least 100,000 y at an AML of 110.5 MTU/acre. Obviously, such a large and persistent dry-out zone will greatly reduce the potential for aqueous-phase transport of radionuclides from a repository. However, use of higher waste loadings also gives rise to extension in both time and space of the
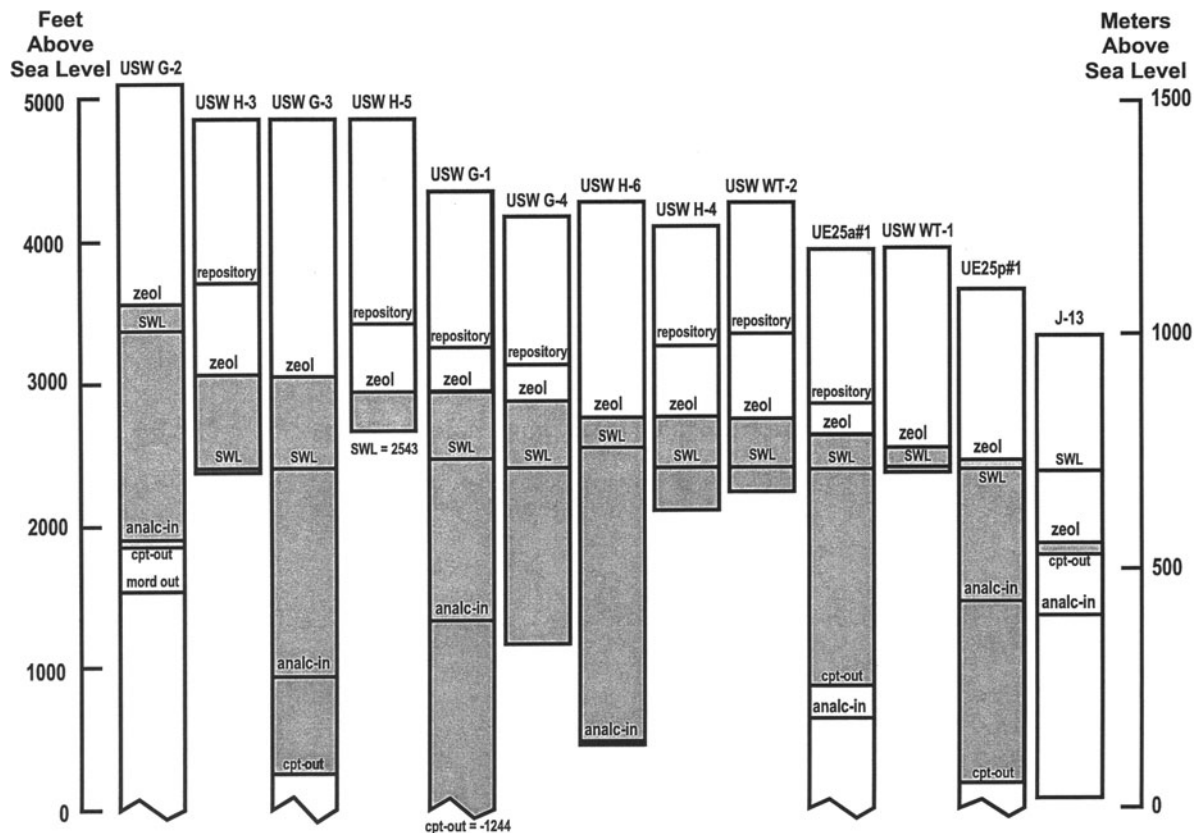
Figure 2.   Drill hole schematic showing the depths of the major zeolitized horizon (diagenetic Zone II—zeol), static water level (SWL), the first occurrence of analcime (diagenetic Zone III—analc-in), and the last occurrence of abundant clinoptilolite (cpt-out) for drill holes shown on Figure 1. Drill holes are shown in order of decreasing elevation of the zeolite horizon. Shaded regions depict the zones in the drill holes in which clinoptilolite-rich horizons occur.

heated region of rock surrounding a repository. Even at the baseline waste loading, zeolitic rocks underlying the repository horizon are predicted to experience temperatures approaching the boiling point of water.

The constraints placed on waste loading by zeolite stability at Yucca Mountain were emphasized as early as 1981 by Smyth and Caporuscio. In a subsequent paper, Smyth (1982) suggested that the sorptive zeolites clinoptilolite and mordenite will be affected under the thermal influence of a repository either by reversible dehydration or by more sluggish mineralogical reactions. The latter include the reaction of clinoptilolite to analcime, evidence of which is seen at depth at Yucca Mountain (Bish and Aronson 1993). Smyth (1982) argued that these reactions could provide both a pathway (shrinkage fractures due to volume reductions) and a driving force (production of water) for release of radionuclides to the biosphere. Based on Yucca Mountain water chemistry and zeolite reaction systematics observed elsewhere, Smyth recommended keeping the zeolite-bearing horizons water saturated and below 85 °C.

Since the stability of clinoptilolite is important in assessing changes in the chemical and bulk-rock properties of Yucca Mountain (water release, sorption, porosity, permeability, change in volume) and thus in radionuclide transport modeling, it is necessary to understand the conditions under which clinoptilolite may react to other phases as a result of repository emplacement. The reaction of clinoptilolite to analcime is important because analcime has a much smaller cation exchange capacity for most radionuclides (Vaughan 1978) and because the reaction gives rise to a net volume decrease of ~17%, assuming the reaction produces quartz as the silica phase. This reduced volume, leading to an increase in porosity, will significantly change the structural and hydraulic properties of the reacted clinoptilolite-bearing units.

Temperatures at which the clinoptilolite-to-analcime reaction has occurred in nature can be approximated by comparing the bottom-hole temperatures obtained from drill holes in Yellowstone National Park (Honda and Muffler 1970; Keith et al. 1978) and the estimated paleogeotherms from Yucca Mountain, Nevada (Bish

1989; Bish and Aronson 1993), with the observed mineral distributions. The data of Honda and Muffler (1970) suggest that the onset of the clinoptilolite-to-analcime reaction occurred in drill hole Y-1 in Yellowstone National Park at approximately 115 °C, although clinoptilolite persisted in the drill hole up to 155 °C. Likewise, Keith et al. (1978) did not report the presence of analcime in drill hole Y-7, even though measured temperatures reached ~135 °C at the bottom of the hole. In drill hole Y-8, however, analcime initially occurs at an interval where the measured temperature is ~80 °C, although clinoptilolite persists in this drill hole to temperatures greater than 160 °C (Keith et al. 1978). The temperature of the clinoptilolite-to-analcime reaction at Yucca Mountain was approximated by comparing the observed mineralogy in drill holes USW G-1, G-2 and G-3 (Bish and Chipera 1989) with the paleogeotherms obtained for the same drill holes calculated using fluid inclusion data and the degree of transformation of smectite to illite (Bish 1989; Bish and Aronson 1993). In the northernmost drill holes, the onset of the clinoptilolite-to-analcime reaction appears to have occurred between approximately 70 and 100 °C, although some clinoptilolite exists to greater depths and higher temperatures. Likewise, mordenite became unstable at temperatures of 100 to 130 °C. However, Bish (1989) and Bish and Aronson (1993) also emphasized that similar mineralogical trends with depth are observed in the southern portion of Yucca Mountain, where temperatures at depth do not appear to have been significantly elevated. Thus, it appears that important zeolite transformations, such as the clinoptilolite-to-analcime reaction, can occur at relatively low temperatures, given appropriate water compositions.

The important effect of water chemistry on zeolite diagenetic reactions was observed during early studies of saline lakes (Hay 1966, 1978; Sheppard and Gude 1968, 1969), in which alkalic, silicic zeolites such as clinoptilolite, erionite or phillipsite often developed on the margins of the deposits, grading into analcime and then into potassium feldspar at the centers of the lakes (for example, the Big Sandy Formation, Sheppard and Gude 1973). It was inferred that the alkalic, silicic zeolites were the first-formed zeolites that subsequently transformed into analcime when the aqueous Na^+ concentration increased as water evaporated. Boles (1971) experimentally reproduced this result by reacting heulandite and clinoptilolite in NaOH and Na_2CO_3 solutions at 100 °C to form analcime. He concluded that the reaction to analcime is favored by increased pH and aqueous Na^+ concentrations and that the Si:Al ratio of the analcime is largely a function of the Si:Al ratio of the precursor zeolite, irrespective of the presence or absence of quartz. The aqueous Na^+ concentrations in the analcime-producing experiments (~2700–4600 ppm) were lower than the concentra-

tions that can occur in modern saline-alkaline lakes (>100,000 ppm Na; Jones et al. 1967; Surdam and Sheppard 1978). Iijima (1975) noted that the clinoptilolite-to-analcime reaction occurred at significantly higher temperatures in marine geosynclinal deposits (~84 to 91 °C) than in the ambient-temperature saline-alkaline lakes. He suggested that the chemical composition of the pore water (in particular the Na^+ concentration) was the primary factor determining reaction temperatures.

In an attempt to evaluate other factors that may control zeolite diagenesis, several investigators have examined the silica polymorphs coexisting with clinoptilolite and analcime (Honda and Muffler 1970; Keith et al. 1978; Kerrisk 1983; Duffy 1993a). Several of these studies suggested that aqueous silica activity, rather than aqueous Na^+ concentration, is the predominant factor controlling the reaction of clinoptilolite to analcime. Clinoptilolite is often observed to coexist with the more soluble silica polymorphs (opal-CT and cristobalite), whereas analcime generally only coexists with quartz (Bish and Chipera 1989). This correlation is documented well in the mineralogic data as a function of depth for drill holes at Yucca Mountain (Bish and Chipera 1989). Equilibrium modeling using EQ3/6 also suggested that high-silica zeolites (clinoptilolite and mordenite) were formed along with smectite during the initial stages of volcanic glass dissolution (Kerrisk 1983). Kerrisk found it necessary to suppress quartz precipitation in his calculations, mimicking the supersaturation of silica, in order to form high-silica zeolites such as clinoptilolite. However, he obtained unrealistic results if cristobalite were also suppressed to allow the silica activity to reach amorphous-silica saturation. If reactions were allowed to continue, silica activity eventually dropped and the reactions progressed to a quartz-analcime-illite assemblage and, finally, to a quartz-albite-potassium feldspar assemblage with possible calcite.

The observed mineral distribution at Yucca Mountain (Bish and Chipera 1989) and the alteration observed in other volcanic ash terrains, such as in Yellowstone National Park (Honda and Muffler 1970; Keith et al. 1978), suggest that the most probable reaction that would lead to destruction of clinoptilolite due to emplacement of a high-level waste repository would be the reaction of clinoptilolite to form analcime. Bowers and Burns (1990) conducted an equilibrium modeling study of the stability of clinoptilolite under current temperature and water chemistry conditions and with respect to potential changes in water chemistry and increased temperature resulting from emplacement of high-level radioactive waste. Bowers and Burns calculated an albite stability field that separated clinoptilolite and analcime. They did not, however, specifically address the clinoptilolite-to-analcime reaction. The present study addresses the stability of

clinoptilolite relative to analcime under current conditions at Yucca Mountain and under conditions that could exist after emplacement of a high-level radioactive waste repository.

METHODS

The thermodynamic calculations in this study used thermodynamic data for zeolites estimated as outlined in Chipera et al. (1995). Various empirical routines have been formulated for estimating thermodynamic data for minerals. Recent methods, however, represent mineral phases as a set of elemental building blocks composed of unique polyhedra (Robinson and Haas 1983; Berman and Brown 1985; Hazen 1985; Chermak and Rimstidt 1989; Holland 1989). By summing the contributions from each polyhedron, the thermodynamic properties can be estimated for the complete mineral unit. In the present study, thermodynamic data for the zeolites were estimated using the methods proposed by Berman and Brown (1985) for heat capacity, Chermak and Rimstidt (1989) for Gibbs free energies and enthalpies of formation at 298 K and Holland (1989) for entropy. Holland's method of estimating entropy from individual polyhedra improves on previous methods by considering phase volumes. This improvement is important, since entropy depends not only on the individual polyhedra comprising the phase, but also on how tightly the polyhedra are assembled. Since Holland proposed only 2 choices for entropy contributions of water in the polyhedrally derived structure (20.74 J/mol·K for structurally bound and 30.03 J/mol·K for "loosely bound" water), a value for "zeolitic" water was determined for the present calculations (in this treatment, "zeolitic" water is more weakly bonded than "loosely bound" water). An average value of 59.1 J/mol·K for zeolitic water was determined by comparing calculated entropies of anhydrous forms of analcime, heulandite, mordenite, phillipsite, clinoptilolite and stilbite (phases representative of those at Yucca Mountain) with the measured hydrous entropy values for these phases (Johnson et al. 1982, 1985, 1992; Hemingway and Robie 1984; Howell et al. 1990) and then determining the average difference on a per-mole-of-water basis. This value (59.1 J/mol·K) compares well with the values measured by others for zeolitic water (55.0 J/mol·K for analcime, Johnson et al. 1982; 57.0 J/mol·K for clinoptilolite, Hemingway and Robie 1984; 54.05 J/mol·K for mordenite, Johnson et al. 1992; and 52.0 J/mol·K for Ca-clinoptilolite, Carey and Bish 1996). The above estimation methods reproduced measured Gibbs free energy and enthalpies of formation at 298 K to within 0.3% (2σ) using the published chemical formulae for analcime, clinoptilolite, heulandite, mordenite and stilbite (GK Johnson et al. 1982, 1985, 1991, 1992; Hemingway and Robie 1984; Howell et al. 1990). Holland's method of estimating entropy re-

produced entropies of analcime, clinoptilolite, heulandite, mordenite, phillipsite and stilbite (GK Johnson et al. 1982, 1985, 1991, 1992; Hemingway and Robie 1984; Howell et al. 1990) to within 4% (2σ) of the measured values using the published chemical formulae.

The primary reason for using estimated thermodynamic data, even though data have now been measured for some clinoptilolite and analcime samples, is that the chemistry of zeolites is highly variable. Thermodynamic properties measured for a zeolite in one sample may not be representative of the thermodynamic properties of the same zeolite from other samples. For example, analcime at Yucca Mountain is more Si-rich (Si:Al ratios of 2.4–2.8) than the analcime used for calorimetric studies (Johnson et al. 1982, Si:Al = 2.15). Recent solubility measurements yielded standard free energies of formation at 25 °C of −3090 ± 5 kJ/mol for a stoichiometric analcime and −3036 ± 5 kJ/mol for an Si-rich sedimentary analcime (Wilkin and Barnes 1995). Likewise, Si:Al ratios for clinoptilolite show considerable variation at Yucca Mountain, ranging from 4 to 5. Clinoptilolite has the added complexity that the exchangeable-cation composition ranges through the Na-Ca-K ternary. Inasmuch as zeolites at Yucca Mountain range widely in chemical composition, some constraints on chemical formulae were imposed using the chemical data from Broxton et al. (1986, 1987). The clinoptilolite/heulandites in diagenetic zone I have uniform Ca-rich compositions (60–90 mol% Ca) and Si:Al ratios mainly between 4.0 and 4.6. Diagenetic Zone-II clinoptilolites, however, show considerably more variability. Clinoptilolites in the eastern part of Yucca Mountain are calcic-potassic, becoming more calcic with depth, whereas clinoptilolites in the western part of Yucca Mountain are sodic-potassic, becoming more sodic with depth. The Si:Al ratios of the Zone-II clinoptilolites are generally between 4.4 and 5.0. In contrast to clinoptilolite, analcime at Yucca Mountain has a more uniform chemical composition consisting of an almost pure Na end member with Si:Al ratios between 2.4 and 2.8, considerably different from stoichiometric end-member analcime (~2.0). Chemical analyses used in the calculations (Broxton et al. 1986) were normalized to form balanced structural formulae when the individual atom abundances were rounded to the first decimal place (Table 1). Thermodynamic data used in the present calculations are shown in Table 2.

Modeling of clinoptilolite-analcime equilibria was conducted assuming the following reaction:

$$s\text{Clinoptilolite} + t\text{Na}^+ \Leftrightarrow$$
$$v\text{Analcime} + w\text{K}^+ + x\text{Ca}^{2+} + y\text{SiO}_2 + z\text{H}_2\text{O}$$
$$[1]$$
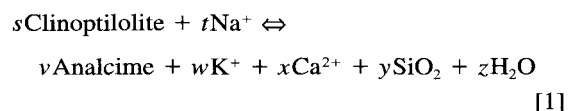
Since thermodynamic data were calculated specifically

Table 1. Chemical formulae of Yucca Mountain clinoptilolites and analcime.

Sample	Label on Fig. 8	Chemical formula	Si:Al ratio	Ca/ (Ca+Na+K)	Na/ (Ca+Na+K)	K/ (Ca+Na+K)
Clinoptilolite						
USW G1-1286	a	$(K_{0.5}Na_{0.9}Ca_{2.7})Al_{6.8}Si_{29.2}O_{72.0} \cdot 26.8H_2O$	4.29	0.66	0.22	0.12
USW G1-1436	b	$(K_{3.3}Na_{2.0}Ca_{0.5})Al_{6.3}Si_{29.7}O_{72.0} \cdot 26.8H_2O$	4.71	0.09	0.34	0.57
USW G1-2166	c	$(K_{2.2}Na_{3.4}Ca_{0.4})Al_{6.4}Si_{29.6}O_{72.0} \cdot 26.8H_2O$	4.63	0.07	0.57	0.37
USW G1-3598	d	$(K_{0.7}Na_{4.3}Ca_{0.9})Al_{6.8}Si_{29.2}O_{72.0} \cdot 26.8H_2O$	4.29	0.15	0.73	0.12
USW G1-3706	e	$(K_{0.3}Na_{3.2}Ca_{1.0})Al_{5.5}Si_{30.5}O_{72.0} \cdot 26.8H_2O$	5.55	0.22	0.71	0.07
USW G2-1691	f	$(K_{2.3}Na_{0.9}Ca_{1.6})Al_{6.4}Si_{29.6}O_{72.0} \cdot 26.8H_2O$	4.63	0.41	0.23	0.59
USW GU3-1874	g	$(K_{2.8}Na_{1.5}Ca_{0.9})Al_{6.1}Si_{29.9}O_{72.0} \cdot 26.8H_2O$	4.90	0.17	0.29	0.54
USW G4-1432	h	$(K_{2.9}Na_{2.1}Ca_{0.7})Al_{6.4}Si_{29.6}O_{72.0} \cdot 26.8H_2O$	4.63	0.12	0.37	0.51
USW H4-1420	i	$(K_{1.9}Na_{0.8}Ca_{1.7})Al_{6.1}Si_{29.9}O_{72.0} \cdot 26.8H_2O$	4.90	0.39	0.18	0.43
USW J13-1421	j	$(K_{2.5}Na_{1.1}Ca_{1.2})Al_{6.0}Si_{30.0}O_{72.0} \cdot 26.8H_2O$	5.00	0.25	0.23	0.52
UE-25p#1-1250	k	$(K_{1.7}Na_{1.0}Ca_{1.8})Al_{6.3}Si_{29.7}O_{72.0} \cdot 26.8H_2O$	4.71	0.40	0.22	0.38
UE-25p#1-3330	l	$(K_{0.4}Na_{1.0}Ca_{3.3})Al_{8.0}Si_{28.0}O_{72.0} \cdot 26.8H_2O$	3.50	0.70	0.21	0.09
Representative analcime		$Na_{10.2}Al_{10.2}Si_{25.8}O_{72.0} \cdot 12H_2O$	2.53	—	1.00	—

for each solid phase and included any variability in exchangeable cation and Si:Al ratios, the activities of both clinoptilolite and analcime were assumed to be 1.0. The calculations were conducted projecting from H_2O (activity = 1), and any reaction or product cations were exchanged with the liquid phase. Note that cation concentrations may be buffered by other reactions occurring in the natural system (such as Ca^{2+} by calcite). The equilibrium constant for the above reaction is approximated as:

$$k = \frac{(aCa^{2+})^x (aK^+)^w (aSiO_2)^y}{(aNa^+)^t}. \quad [2]$$

As is obvious from the equilibrium constant, cation concentrations and aqueous silica activity both affect calculated equilibria.

Thermodynamic calculations in this study were conducted using the Ge0-Calc PTA-SYSTEM software (Brown et al. 1989). Ge0-Calc runs on a personal computer (PC) and allows rapid calculation of thermodynamic stability fields under conditions of variable temperature, pressure or activities of phases involved in the reactions. In addition, Ge0-Calc balances complex chemical reactions, a desirable feature when using actual chemical analyses which can deviate significantly from stoichiometric "ideal" formulae. Thermodynamic data for quartz, cristobalite and tridymite were obtained from the B88.MIN thermodynamic database

Table 2. Estimated thermodynamic data for clinoptilolite and a representative Yucca Mountain analcime.

Sample	ΔG_f°† (kJ/mol)	ΔH_f°† (kJ/mol)	S°‡ (J/mol·K)	Volume§ (cm³/mol)	k_0¶ $\times 10^0$	k_1¶ $\times 10^{-2}$	k_2¶ $\times 10^{-5}$	k_3¶ $\times 10^{-7}$
Clinoptilolite								
USW G1-1286	−39312.0	−42749.5	3123.9	1264.1	5671.83	−386.73	−920.81	1306.10
USW G1-1436	−39150.9	−42561.6	3216.7	1264.1	5743.54	−390.01	−949.80	1374.71
USW G1-2166	−39149.2	−42556.5	3220.2	1264.1	5745.27	−386.52	−985.34	1433.56
USW G1-3598	−39249.4	−42659.3	3206.0	1264.1	5735.39	−383.06	−100.76	1464.65
USW G1-3706	−38855.7	−42278.9	3152.0	1264.1	5681.18	−383.14	−981.89	1423.54
USW G2-1691	−39196.9	−42622.7	3166.5	1264.1	5704.06	−389.64	−921.54	1318.13
USW GU3-1874	−39093.8	−42512.1	3189.1	1264.1	5719.64	−389.66	−937.40	1351.00
USW G4-1432	−39178.2	−42590.7	3209.6	1264.1	5738.34	−389.25	−952.17	1376.57
USW H4-1420	−39101.1	−42531.0	3149.2	1264.1	5687.34	−388.95	−919.54	1314.34
USW J13-1421	−39067.7	−42491.3	3170.7	1264.1	5703.97	−389.58	−927.38	1331.96
UE-25p#1-1250	−39159.5	−42588.8	3151.2	1264.1	5690.36	−388.46	−924.28	1320.87
UE-25p#1-3330	−39689.6	−43125.1	3140.5	1264.1	5695.47	−386.95	−921.17	1299.42
Representative analcime	−36660.3	−39247.6	2664.2	1168.1	4593.9	−264.11	−115.19	1696.32

† Gibbs free energies and enthalpies of formation estimated using Chermak and Rimstidt (1989).
‡ Entropies estimated using Holland (1989).
§ Molar volumes from Smyth and Bish (1988).
¶ Heat capacity terms for equation $C_p = k_0 + k_1 T^{-0.5} + k_2 T^{-2} + k_3 T^{-3}$ in units of J/mol·K estimated using Berman and Brown (1985).
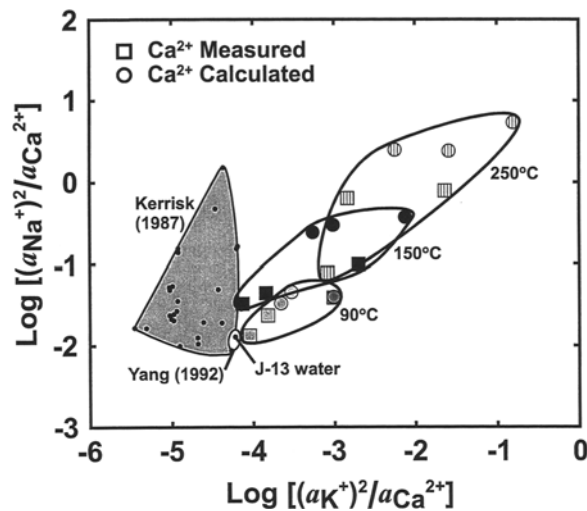
Figure 3. Yucca Mountain water compositions, including analyses from drill holes in the vicinity of Yucca Mountain (Kerrisk 1987), well J-13 water (Delany 1985), pore water obtained from Topopah Spring Tuff (Yang 1992) and projected water compositions using J-13 water equilibrated with Topopah Spring Tuff samples at elevated temperatures (Delany 1985; Knauss, Beiriger and Peifer 1985, 1987; Knauss, Beiriger, Peifer and Piwinskii 1985; Knauss and Peifer 1986). Gray shading depicts the 90-°C data, black depicts the 150-°C data and striped depicts the 250-°C data. The data obtained from the LLNL experiments using measured pH are shown as squares. Circles show water compositions revised using Ca-concentrations that we calculated from calcite equilibria using a fixed J-13 water pH of 7.6 and the measured HCO_3^- from the LLNL experiments.

(Berman 1988) supplied with the Ge0-Calc software package. Likewise, values for aqueous species (aqueous SiO_2, Ca^{2+}, Na^+, K^+, H^+) were taken from the HKF81.AQU database (Helgeson et al. 1981) also supplied with the Ge0-Calc software. The Ge0-Calc databases, however, do not supply thermodynamic data for amorphous silica which, for this study, were obtained from the SUPCRT92 database (JW Johnson et al. 1991). To simplify the calculations, the chemical system was constrained to the system Na-K-Ca-Al-Si-O-H.

In addition to exchangeable- and tetrahedral-cation compositional variability, zeolites exhibit wide variations in water content, readily responding to changes in temperature and humidity. For the present calculations, all zeolites were assumed to be fully hydrated, as would be expected of a zeolite below the water table or at 100% relative humidity. The exact amount of water an individual zeolite contains, however, is strongly dependent on the exchangeable cations in the zeolite structure and on the total abundance of cations in the zeolite. For example, under given temperature and humidity conditions, more water will be incorporated in Ca-clinoptilolite/heulandites than in Na- or K-clinoptilolite/heulandites due to the greater hydra-

tion energy of Ca^{2+} and the greater number of sites available in the extraframework cavities (Bish 1988). For example, chemical analyses show that heulandite typically contains more water than clinoptilolite (Gottardi and Galli 1985). Scoping calculations conducted using a constant clinoptilolite chemical formula but varying the water content showed that reducing the water content in clinoptilolite increased the stability of clinoptilolite with respect to analcime. However, although Carey and Bish (1996) presented data which show that Ca-clinoptilolite may lose up to 30% of its water at 1 bar total pressure and 150 °C, conditions that may exist in a repository environment, we have ignored dehydration to obtain conservative results.

In the present calculations, initial cation concentrations in the fluid phase were assumed to approximate the current concentrations measured in Yucca Mountain ground water (Kerrisk 1987; Perfect et al. 1995). Pressure was constrained such that all calculations were conducted on the liquid side of the water liquid-vapor curve. Additional calculations performed at 1 to 200 bar showed that these low pressures have an insignificant effect on clinoptilolite/analcime equilibria.

RESULTS AND DISCUSSION

In order to understand the conditions that may affect clinoptilolite-analcime equilibria during the life of a high-level radioactive waste repository, it is necessary to know the current water compositions at Yucca Mountain and to predict changes in water chemistry in response to heating by the potential repository. Figure 3 shows the Na, Ca and K concentrations in a $log[(aK^+)^2/aCa^{2+}]$ versus $log[(aNa^+)^2/aCa^{2+}]$ diagram from drill holes in the vicinity of Yucca Mountain (Kerrisk 1987). The Yucca Mountain Project typically uses water from the J-13 water-supply well as an analog to the water in the Topopah Spring Tuff, the unit in which the repository horizon may be located. Well J-13 is the producing well nearest to Yucca Mountain, and its major producing horizon is a highly fractured interval within the Topopah Spring Tuff. For comparison, the pore-water compositions in the unsaturated Topopah Spring Tuff obtained by Yang (1992) are also plotted on Figure 3. To estimate the changes in groundwater chemistry that may result from repository-induced heating, investigators from the Lawrence Livermore National Laboratory (LLNL) reacted J-13 water with samples of Topopah Spring Tuff (crushed devitrified tuff, wafers of devitrified tuff, and wafers of vitric tuff) at 90, 150 and 250 °C (Delany 1985; Knauss, Beiriger and Peifer 1985, 1987; Knauss, Beiriger, Peifer and Piwinskii 1985; Knauss and Peifer 1986). The concentrations of Na^+, K^+ and HCO_3^- increased slightly, whereas Ca^{2+} and Mg^{2+} decreased significantly in concentration due to their removal as carbonate phases (Figure 3). The pH also decreased during the hydrothermal experiments. However, sev-
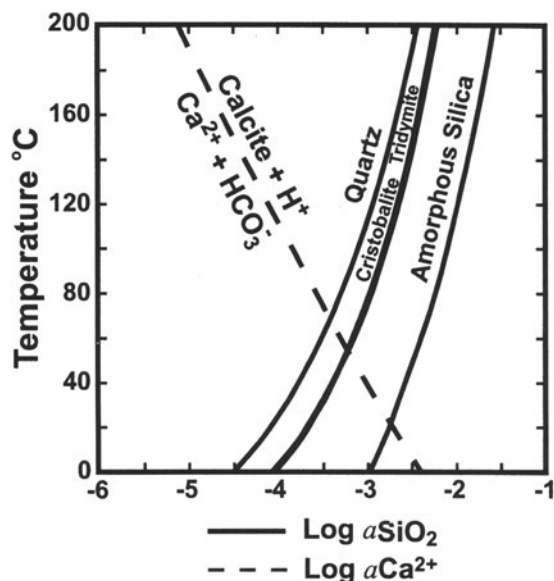
Figure 4. Effects of temperature on silica activity for various silica polymorphs and on Ca activity in equilibrium with calcite. Cristobalite and tridymite have similar solubilities. Calcite equilibria were calculated using a pH of 7.6 and $pHCO_3^-$ of 2.7.

Figure 5. $Log[(aNa^+)^2/aCa^{2+}]$ vs. $log(aSiO_2)$ diagram showing the effects of variable clinoptilolite Si:Al ratio on clinoptilolite-analcime equilibria at 100 °C. Calculations varied the Si:Al ratio in clinoptilolite, assuming a generalized formula of $(Ca=Na)_{2/3x}Al_xSi_{36-x}O_{72} \cdot 26.8H_2O$. Shaded area shows the average Yucca Mountain clinoptilolite Si:Al ratios. Present Yucca Mountain water compositions (Kerrisk 1987) and quartz (Qtz) and cristobalite (Crst) solubilities at 100 °C are shown for reference.

eral studies suggest that the dominant effect of repository heating of Yucca Mountain would be the volatilization of CO_2 accompanied by increasing pH and precipitation of calcite, which would be limited only by the amount of Ca^{2+} present to form calcite (Codell and Murphy 1992; Murphy 1994; Murphy and Pabalan 1994). Even if pH were to remain constant, calculated Ca^{2+} concentrations would be significantly lower than those obtained in the LLNL experiments, as shown in Figure 3. During the LLNL experiments, silica activity increased through dissolution of silica polymorphs and glass to levels that were at or above cristobalite solubility. This increase occurred because the equilibrium aqueous silica concentration of each silica polymorph is strongly affected by temperature. The effects of increasing temperature on aqueous Ca and silica concentrations are illustrated in Figure 4. It should also be noted that the LLNL experiments were conducted at high water-to-rock ratios that would be representative of the saturated zone but may not be representative of reactions occurring under unsaturated conditions in the vadose zone.

The effect of variable clinoptilolite Si:Al ratio on equilibria with analcime was modeled using a fixed, representative Yucca Mountain analcime composition but varying the Si:Al ratio in clinoptilolite (Figure 5). The ratio of Na:Ca in clinoptilolite was held at 1:1, although the total moles of Ca plus Na were varied to charge-balance the variable Si:Al. These calculations demonstrate that equilibria involving siliceous clinoptilolites are sensitive to aqueous silica activity. Equi-
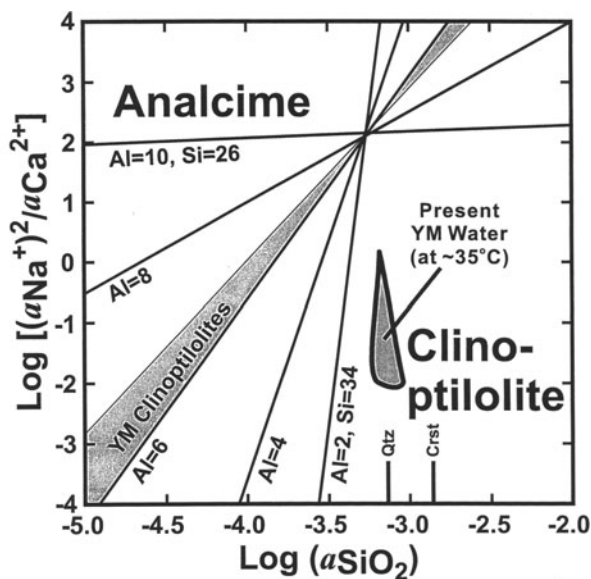
libria involving aluminous clinoptilolite/heulandite are less sensitive to aqueous silica activity but are more sensitive to the aqueous Na:Ca ratio. For reference, the Si:Al ratios observed for Yucca Mountain clinoptilolites are shown in the shaded region on Figure 5. Varying the Si:Al ratio in analcime within values representative of those at Yucca Mountain resulted in insignificant changes to the equilibria in Figure 5.

The effects of Na:Ca ratio in clinoptilolite on equilibria with analcime were modeled in a manner similar to the above calculations, except that Na:Ca ratio was allowed to vary and the Si:Al ratio was fixed at 4.45 (a representative value for Yucca Mountain clinoptilolites). Figure 6 shows that Na-clinoptilolite is more sensitive to the aqueous silica activity and less sensitive to the aqueous Na:Ca ratio than Ca-clinoptilolite, since Na-clinoptilolite can react directly to form Na-analcime. Ca-clinoptilolites are much more sensitive to the aqueous Na:Ca ratio, requiring a substantially higher ratio for analcime formation. Thus, for this particular clinoptilolite Al:Si ratio, increasing the clinoptilolite Ca content expands the clinoptilolite stability field at silica activities $<10^{-3.2}$ and decreases the stability field at silica activities $>10^{-3.2}$. However, it is important to note that the aqueous Na:Ca ratio must be at least 3 orders of magnitude greater than what occurs currently at Yucca Mountain (Kerrisk 1987) to reach the "crossover point" for this clinoptilolite. The
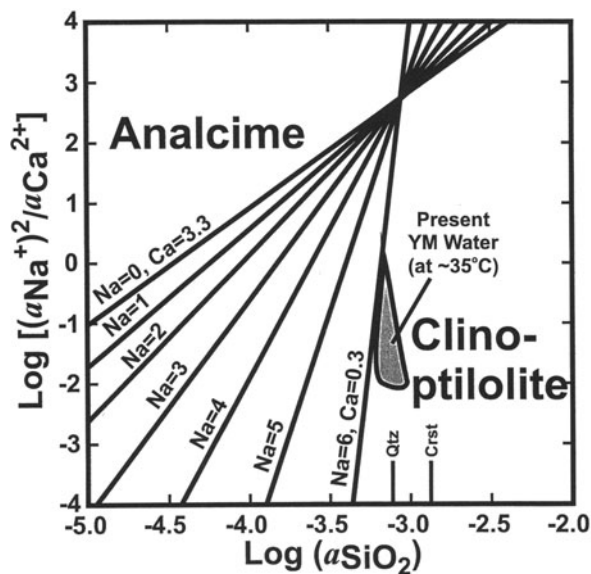
Figure 6.   Log$[(a\text{Na}^+)^2/a\text{Ca}^{2+}]$ vs. log$(a\text{SiO}_2)$ diagram showing the effects of variable clinoptilolite Ca:Na ratio on clinoptilolite-analcime equilibria at 100 °C. Calculations varied the Ca:Na ratio in clinoptilolite assuming a generalized formula of $(\text{Ca},\text{Na})_x\text{Al}_{6.6}\text{Si}_{29.4}\text{O}_{72}\cdot26.8\text{H}_2\text{O}$. Present Yucca Mountain water compositions (Kerrisk 1987) and quartz (Qtz) and cristobalite (Crst) solubilities at 100 °C are shown for reference.
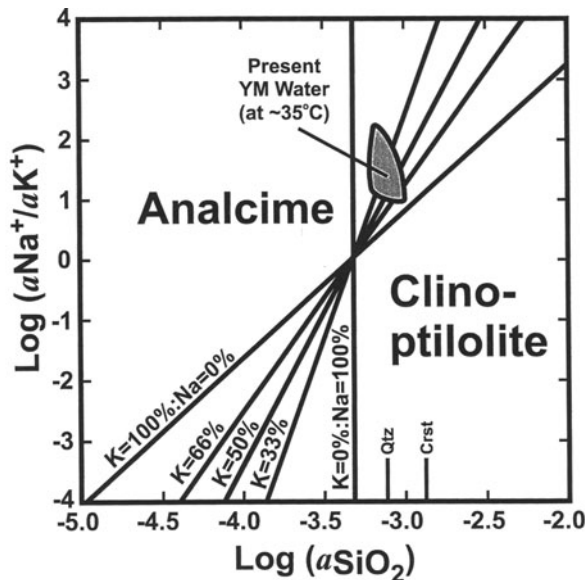
Figure 7.   Log$(a\text{Na}^+/a\text{K}^+)$ vs. log$(a\text{SiO}_2)$ diagram showing the effects of clinoptilolite K:Na ratio on clinoptilolite-analcime equilibria at 100 °C. Calculations varied the K:Na ratio in clinoptilolite assuming a generalized formula of $(\text{K},\text{Na})_{6.6}\text{Al}_{6.6}\text{Si}_{29.4}\text{O}_{72}\cdot26.8\text{H}_2\text{O}$. Present Yucca Mountain water compositions (Kerrisk 1987) and quartz (Qtz) and cristobalite (Crst) solubilities at 100 °C are shown for reference.

exact location of the "crossover point" depends on the chemical compositions of clinoptilolite and analcime used in the calculations. The effects of Na:K composition in clinoptilolite on equilibria with analcime (Figure 7) were modeled in the same manner as the Na:Ca compositions. Although clinoptilolite-analcime equilibria are similar to those obtained for the Na:Ca system, present Yucca Mountain water compositions (Kerrisk 1987) plot on the opposite side of the "crossover point." Therefore, increases in aqueous K concentration increase the stability of clinoptilolite with respect to analcime, but increases in clinoptilolite K content decrease clinoptilolite stability.

Using the constraints outlined above, calculations were performed using observed chemical formulae for Yucca Mountain clinoptilolites and a representative chemical formula for Yucca Mountain analcime (Table 1). The 12 clinoptilolites used in the calculations were selected to represent the observed variation in chemical compositions, both in exchangeable-cation ratios and in Si:Al ratios. Log$[(a\text{K}^+)^2/a\text{Ca}^{2+}]$ versus log$[(a\text{Na}^+)^2/a\text{Ca}^{2+}]$ diagrams showing clinoptilolite-analcime equilibria are shown in Figures 8a–d. The phase boundary for each of the 12 clinoptilolite compositions is portrayed as a line in Figures 8a–d, where clinoptilolite is stable below that line and analcime is stable above. Figures 8a and 8c show equilibria calculated at cristobalite saturation at 100 and 150 °C. Assuming J-13 water composition, clinoptilolite is the

stable phase with respect to analcime for all 12 clinoptilolite compositions at cristobalite saturation and 100 °C. However, when temperature was increased to 150 °C, several clinoptilolite/analcime equilibria shifted below the Yucca Mountain water compositions on Figure 8c, thereby shifting the stability field for several clinoptilolite compositions to analcime. Likewise, Figures 8b and 8d show the results for the 12 clinoptilolites at 100 and 150 °C with a silica activity in equilibrium with quartz. The effect of decreasing the aqueous silica activity was to shift the equilibria further, with several additional clinoptilolite/analcime equilibria shifting below the Yucca Mountain water compositions on Figures 8b and 8d. At 150 °C, with an aqueous silica activity in equilibrium with quartz and assuming J-13 water composition (Figure 8d), approximately half of the clinoptilolite/analcime equilibria shift such that analcime would be stable in the Yucca Mountain waters. Since the chemical composition of Yucca Mountain analcime is fairly constant, the effect of varying the analcime Si:Al ratio within the limits observed at Yucca Mountain shifted the equilibria only slightly at all silica activities and temperatures. It is *important to note that, although J-13 water and the pore water chemistry* (Yang 1992) are considered representative of water in the Topopah Spring Tuff, other water compositions measured at Yucca Mountain (Kerrisk 1987) result in significantly reduced stability fields for clinoptilolite. Thus, for example, assuming
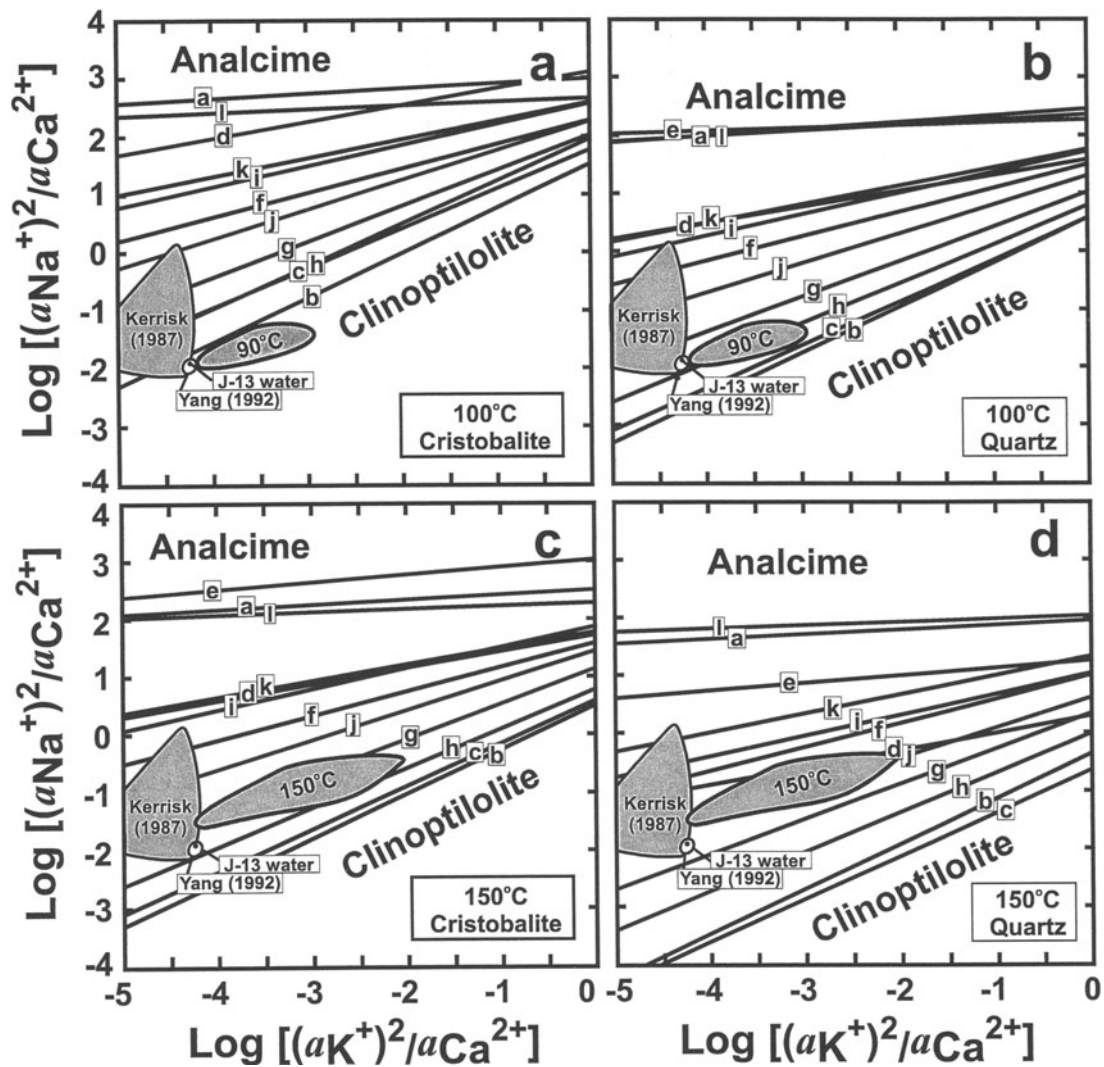
Figure 8. Log[$(aNa^+)^2/aCa^{2+}$] vs. log[$(aK^+)^2/aCa^{2+}$] diagrams showing equilibria of 12 Yucca Mountain clinoptilolites exhibiting a representative range of exchangeable-cation and Si:Al ratios (Table 1). Calculations assumed temperatures of 100 and 150 °C and silica activities in equilibrium with cristobalite or quartz. Chemical compositions of J-13 water, measured pore water composition from Yang (1992), projected 90 and 150 °C J-13 water compositions (Delany 1985; Knauss, Beiriger and Peifer 1985, 1987; Knauss, Beiriger, Peifer and Piwinskii 1985; Knauss and Peifer 1986) and the chemical analyses of Yucca Mountain waters from Kerrisk (1987) are plotted on the figures for reference.

the Na-rich water composition of Kerrisk (1987) at 100 or 150 °C in equilibrium with quartz, stability fields for clinoptilolite exist for only a few clinoptilolite compositions (Figures 8b and 8d).

The thermodynamic calculations show that silica activity, temperature and the concentration of K, Na and Ca in both clinoptilolite and in ground water are all important in determining clinoptilolite-analcime equilibria. Although the measured cation ratios in clinoptilolite were used in these calculations, clinoptilolite is well recognized for its cation exchange capability. For example, based on measured compositions of water migrating through fractures at Rainier Mesa (~50 km north-northeast of Yucca Mountain), White et al.

(1980) concluded that water compositions in fractures are controlled mainly by dissolution of vitric tuff but are modified during infiltration through zeolitized tuffs. Thus the existing exchangeable-cation ratios in clinoptilolite may well change in response to an increase in temperature and/or a change in water chemistry. The selectivity of clinoptilolite for various alkali and alkaline-earth cations has been well documented since the early studies by Ames (1964a, 1964b). However, cation exchange is not a straightforward process in clinoptilolite; it is a function of several factors including the cation species, the selectivity of each exchange site for a particular cation, the temperature at which the exchange occurs and the ionic strength of

the exchange solution. Unfortunately, reliable data at elevated temperatures and in multicomponent systems do not exist, although several generalizations can be drawn from the available literature to predict cation exchange in clinoptilolite under conditions resulting from potential emplacement of a waste repository. At low ionic strengths, clinoptilolite has a greater affinity for divalent versus monovalent cations (Barrer and Klinowski 1974; Pabalan and Murphy 1990; Bruton et al. 1993; Pabalan and Bertetti 1994). Thus, at the ionic strengths present at Yucca Mountain, clinoptilolite has a strong preference for Ca^{2+} over Na^+. For a given clinoptilolite, a large increase in aqueous Na^+ concentration will give rise to a smaller increase in the amount of Na^+ in clinoptilolite. Bruton et al. (1993) also concluded that the selectivity of clinoptilolite for Ca^{2+} increases with increasing temperature. Thus, for a given water composition, Yucca Mountain clinoptilolites will tend to be enriched in Ca^{2+} as temperature increases. Ultimately, the extent to which clinoptilolite-bearing horizons in Yucca Mountain will alter the water chemistry or vice versa will depend on the clinoptilolite-to-groundwater ratio in addition to the clinoptilolite and water chemistry.

It is useful to compare these modeling results with the information obtained on zeolite stability at Yucca Mountain. Bish and Aronson (1993) suggested that the clinoptilolite reacted to form analcime in drill hole USW G-2, in the northern end of Yucca Mountain, at temperatures of 70 to 100 °C. However, these high temperatures were not attained in drill hole USW G-3, much farther to the south, but clinoptilolite-bearing assemblages nevertheless grade into analcime-bearing assemblages with depth in that drill hole. Data presented in Broxton et al. (1987) show a trend in clinoptilolite compositions at Yucca Mountain where, with increasing depth, clinoptilolite compositions on a ternary diagram migrate away from the K-apex toward the Na-apex in the western part of Yucca Mountain and toward the Ca+Mg apex in the eastern part of Yucca Mountain. Also, the water in western Yucca Mountain is Na-rich relative to water in eastern Yucca Mountain, which is K-rich. Since drill hole USW G-3 is in the western domain, it appears that the Na-K-Ca ratios in both clinoptilolite and groundwater may have been at least partly responsible for the reaction of clinoptilolite to analcime in that drill hole at comparatively low temperatures.

Likewise, reduction in the aqueous silica activity appears to have affected the clinoptilolite-to-analcime reaction at Yucca Mountain. Using water chemistry from packed off zones in several drill holes at Yucca Mountain, Duffy (1993a) noted that, although solubility of a given silica polymorph increases with temperature (Figure 4), the deeper, hotter water samples from these drill holes show consistently lower dissolved silica concentrations than do the cooler, shallower sam-

ples. Reduction in aqueous silica activity with depth, accompanying the change in silica polymorphs, undoubtedly affected clinoptilolite-analcime equilibria in drill hole USW G-3. Clinoptilolite persists to depths greater than the deepest occurrence of opal-CT or cristobalite in many drill holes (USW G-1, USW G-3, USW G-4, UE-25blh, UE-25p#1) and thus probably exists at an aqueous silica activity in equilibrium with the abundant quartz at depth in those drill holes. Although an aqueous silica activity equal to or greater than cristobalite saturation stabilizes clinoptilolite, it appears that reduction in the aqueous silica activity to that of quartz saturation, although generally stabilizing analcime, did not automatically result in conversion of all clinoptilolite to analcime at Yucca Mountain. This effect is illustrated well by Figures 8b and 8d, showing that several clinoptilolite compositions are stable with respect to analcime at 100 and 150 °C in Yucca Mountain waters at an aqueous silica activity in equilibrium with quartz.

Because zeolite reactions at Yucca Mountain are so strongly tied to the aqueous silica activity, it is important to consider not only the zeolite reactions themselves but also the kinetics of reactions that would give rise to a change in the aqueous silica activity, such as the transformation of tridymite, cristobalite and opal-CT to quartz. Duffy (1993a) modeled the conversion of these more soluble silica polymorphs to quartz at various depths in drill hole USW G-1 using the time/temperature predictions of Johnstone et al. (1984) and the silica transformation models outlined in Duffy (1993b). His models predicted an increase in the amount of quartz but incomplete conversion of the more soluble silica polymorphs over the 100,000-y time span used in the calculation. Consequently, Duffy (1993a) concluded that the aqueous silica activity in rocks presently containing significant tridymite, cristobalite, opal-CT or glass will remain at or above cristobalite saturation over the proposed lifetime of the repository.

The zeolite distributions observed at Yucca Mountain (Bish and Chipera 1989) and also in the altered volcanic rocks at Yellowstone National Park (Honda and Muffler 1970; Keith et al. 1978) suggest that the clinoptilolite-to-analcime reaction does not occur as a sharp, well-defined transition as a function of depth or temperature. Clinoptilolite/heulandite and analcime can and do coexist in the same sample, often to depths well beyond the first occurrence of analcime. To determine the nature of clinoptilolite/heulandite coexisting with analcime at depth in drill hole UE-25p#1, Chipera and Bish (1988) concentrated the zeolite fraction from drill-cuttings at a depth interval of 1061/1064 m (3480/3490 ft) using sodium polytungstate heavy liquids. The clinoptilolite/heulandite in this interval occurs 536 m (1760 ft) below the deepest confirmed occurrence of opal-CT or cristobalite, suggest-

ing that the aqueous silica activity is in equilibrium with the abundant quartz. In addition, the temperature appears to have been greater than 100 °C, as suggested by the presence of an R1 illite/smectite (allevardite; Perry and Hower 1970) in that interval of the drill hole. The zeolite concentrate was analyzed using X-ray powder diffraction (XRD), was placed in a 450 °C oven for 16 h, and then reanalyzed by XRD to determine the thermal stability of the clinoptilolite/heulandite component as outlined by Mumpton (1960) (clinoptilolite is stable to 750 °C, whereas heulandite becomes amorphous when heated for 16 h at 450 °C). The clinoptilolite-group diffraction pattern completely disappeared upon heating, confirming that the zeolite in this sample was heulandite. Other clinoptilolite/heulandite minerals coexisting with analcime at depth in Yucca Mountain are probably also heulandite as suggested by the thermodynamic calculations conducted in this study. Observations of mineralogic relations at Yucca Mountain broadly agree with the trends predicted by the present thermodynamic calculations.

SUMMARY AND CONCLUSIONS

Using estimated thermodynamic data and actual chemical compositions of clinoptilolite and analcime at Yucca Mountain, Nevada, $\log[(a\mathrm{K}^+)^2/a\mathrm{Ca}^{2+}]$ vs. $\log[(a\mathrm{Na}^+)^2/a\mathrm{Ca}^{2+}]$ diagrams were calculated to depict clinoptilolite-analcime equilibria at several temperatures and aqueous silica activities. Temperature, relative cation abundances and aqueous silica activity are all important factors in determining clinoptilolite-analcime equilibria. Increased Na^+ concentrations in either clinoptilolite or the fluid phase, increased clinoptilolite K^+ concentration, increased temperature and decreased aqueous silica activity all stabilize analcime relative to clinoptilolite, assuming present-day Yucca Mountain water compositions. However, increased Ca^{2+} concentrations in either clinoptilolite or the fluid phase, increased aqueous K^+ concentration, and increased Al:Si ratios in clinoptilolite (heulandite) all stabilize clinoptilolite with respect to analcime.

In the vicinity of the repository horizon in the lower portion of the Topopah Spring Tuff, diagenetic Zone-I clinoptilolites are calcic and have high Al:Si ratios (they resemble heulandite). Their particular chemical compositions thus favor their stability relative to analcime under potential repository conditions. Although a decrease in aqueous silica activity tends to stabilize analcime with respect to clinoptilolite, such a decrease will not necessarily be encountered over the lifetime of a repository, since the rocks in proximity to the repository horizon are rich in unaltered glass, cristobalite and tridymite. As long as these silica phases are present, the silica activity should persist at levels at or above equilibrium with cristobalite. However, an important caveat must be applied when considering reactions around the potential repository. The reactions

described in this paper implicitly assume the presence of saturated conditions. Thus, they require either the presence of local saturation or the improbable elevation of the SWL. Reactions occurring with clinoptilolite under dry conditions involve dehydration and cation migration (Bish 1990) and do not lead to the formation of higher-temperature hydrous phases such as analcime. It is unclear what the extent of mineral reaction would be under partially saturated conditions, but it seems probable that mineral reactions would be distinct from those discussed here. Although low $P(\mathrm{H_2O})$ generally stabilizes the less hydrous phase, the lack of sufficient water to provide for mass transfer will probably preclude the formation of analcime under nonsaturated hydrologic conditions.

The temperatures experienced by clinoptilolite-bearing horizons at Yucca Mountain are dependent on the thermal load scenario, but clinoptilolite should remain stable if temperatures in these horizons do not significantly exceed 100 °C, assuming J-13 water chemistry. Even if temperatures rise significantly (for example, to 150 °C), not all clinoptilolite is likely to alter to analcime. Perhaps more importantly, thermodynamic modeling results show that some Yucca Mountain clinoptilolites may remain stable at elevated temperatures, even with an aqueous silica activity at quartz saturation. This conclusion is supported by the occurrence of heulandite coexisting with analcime at considerable depth in drill hole UE-25p#1 (1061/1064 m) in rocks that have apparently experienced temperatures of at least 100 °C. These results differ from previous published results suggesting that clinoptilolite is stable only with an aqueous silica activity at or above cristobalite saturation. Although the results of this study suggest that some clinoptilolites may be stable at 150 °C with an aqueous silica activity at quartz saturation and at fluid compositions approximated by J-13 water, the actual stability may be reduced in nature due to changes in water composition in response to temperature and other external conditions. In addition, cation exchange may also affect clinoptilolite/analcime equilibria. Since the stability of clinoptilolite is dependent on the chemistry of the water with which it is in contact, the effects of materials used in construction of a repository may also change the local water chemistry and could significantly affect clinoptilolite-analcime equilibria.

ACKNOWLEDGMENTS

REFERENCES

Ames LL Jr. 1964a. Some zeolite equilibria with alkali metal cations. Am Mineral 49:127–145.

Ames LL Jr. 1964b. Some zeolite equilibria with alkaline earth metal cations. Am Mineral 49:1099–1110.

Barrer RM, Klinowski J. 1974. Ion-exchange selectivity and electrolyte concentration. J Chem Soc Faraday Trans 70: 2080–2091.

Berman RG. 1988. Internally consistent thermodynamic data for minerals in the system Na_2O-K_2O-CaO-MgO-FeO-Fe_2O_3-Al_2O_3-SiO_2-TiO_2-H_2O-CO_2. J Petrol 29:445–522.

Berman RG, Brown TH. 1985. Heat capacity of minerals in the system Na_2O-K_2O-CaO-MgO-FeO-Fe_2O_3-Al_2O_3-SiO_2-TiO_2-H_2O-CO_2: Representation, estimation, and high temperature extrapolation. Contrib Mineral Petrol 89:168–183.

Bish DL. 1988. Effects of composition on the dehydration behavior of clinoptilolite and heulandite. In: Kallo D, Sherry HS, editors. Occurrence, properties and utilization of natural zeolites. Budapest: Akademiai Kiado. p 565–576.

Bish DL. 1989. Evaluation of past and future alterations in tuff at Yucca Mountain, Nevada, based on the clay mineralogy of drill cores USW G-1, G-2, and G-3. Los Alamos National Laboratory Report LA-10667-MS. 40 p.

Bish DL. 1990. Long-term thermal stability of clinoptilolite: The development of a "B" phase. Eur J Mineral 2:771–777.

Bish DL, Aronson JL. 1993. Paleogeothermal and paleohydrologic conditions in silicic tuff from Yucca Mountain, Nevada. Clays Clay Miner 41:148–161.

Bish DL, Chipera SJ. 1989. Revised mineralogic summary of Yucca Mountain, Nevada. Los Alamos National Laboratory Report LA-11497-MS. 68 p.

Boles JR. 1971. Synthesis of analcime from natural heulandite and clinoptilolite. Am Mineral 56:1724–1734.

Bowers TS, Burns RG. 1990. Activity diagrams for clinoptilolite: Susceptibility of this zeolite to further diagenetic reactions. Am Mineral 75:601–619.

Brown TH, Berman RG, Perkins EH. 1989. PTA-SYSTEM: A Ge0-Calc software package for the calculation and display of activity-temperature-pressure phase diagrams. Am Mineral 74:485–487.

Broxton DE, Bish DL, Warren RG. 1987. Distribution and chemistry of diagenetic minerals at Yucca Mountain, Nye County, Nevada. Clays Clay Miner 35:89–110.

Broxton DE, Warren RG, Hagan RC, Luedemann G. 1986. Chemistry of diagenetically altered tuffs at a potential nuclear waste repository, Yucca Mountain, Nye County, Nevada. Los Alamos National Laboratory Report LA-10802-MS. 160 p.

Bruton C, Glassley WE, Viani BE. 1993. Geochemistry. In: Wilder DG, editor. Preliminary near-field environment report, volume II: Scientific overview of near-field environment and phenomena. Lawrence Livermore National Laboratory Report UCRL-LR-107476 vol 2. 37:122.

Buscheck TA, Nitao JJ, Saterlie SF. 1994. Evaluation of thermo-hydrological performance in support of the thermal loading systems study. High Level Radioactive Waste Management, Proc 5th Annu Int Conf, vol 2; 22-26 May 1994; Las Vegas, NV. p 592–610.

Carey JW, Bish DL. 1996. Equilibrium in the clinoptilolite-H_2O system. Am Mineral 81:952–962.

Chermak JA, Rimstidt JD. 1989. Estimating the thermodynamic properties (ΔG_f^o and ΔH_f^o) of silicate minerals at 298 K from the sum of polyhedral contributions. Am Mineral 74:1023–1031.

Chipera SJ, Bish DL. 1988. Mineralogy of drill hole UE-25p#1 at Yucca Mountain, Nevada. Los Alamos National Laboratory Report LA-11292-MS. 24 p.

Chipera SJ, Bish DL, Carlos BA. 1995. Equilibrium modeling of the formation of zeolites in fractures at Yucca Mountain, Nevada. In: Ming DW, Mumpton FA, editors. Natural zeolites '93: Occurrence, properties, use. Brockport, NY: Int Committee on Natural Zeolites. p 565–577.

Codell RB, Murphy WM. 1992. Geochemical model for 14C transport in unsaturated rock. Proc 3rd Annu High Level Radioactive Waste Management Meeting; Las Vegas, NV. 1959–1965.

Delany JM. 1985. Reactions of Topopah Spring Tuff with J-13 water: A geochemical modeling approach using the EQ3/6 reaction path code. Lawrence Livermore National Laboratory Report UCRL-53631. 46 p.

Duffy CJ. 1993a. Preliminary conceptual model for mineral evolution in Yucca Mountain. Los Alamos National Laboratory Report LA-12708-MS. 46 p.

Duffy CJ. 1993b. Kinetics of silica-phase transitions. Los Alamos National Laboratory Report LA-12564-MS. 22 p.

Gottardi G, Galli E. 1985. Natural zeolites. New York: Springer-Verlag. 409 p.

Hay RL. 1966. Zeolites and zeolitic reactions in sedimentary rocks. Geol Soc Am Spec Pap 85. 130 p.

Hay RL. 1978. Geologic occurrence of zeolites. In: Sand LB, Mumpton FA, editors. Natural zeolites: Occurrence, properties, use. New York: Pergamon Pr. p 135–143.

Hazen RM. 1985. Comparative crystal chemistry and the polyhedral approach. In: Kieffer SW, Navrotsky A, editors. Microscopic to macroscopic: Atomic environments to mineral thermodynamics. Rev Mineral 14. Washington DC: Mineral Soc Am. p 317–345.

Helgeson HC, Kirkham DH, Flowers GC. 1981. Theoretical prediction of the thermodynamic behavior of aqueous electrolytes at high pressures and temperatures: IV. Calculation of activity coefficients, osmotic coefficients, and apparent molal and standard and relative partial molal properties to 600°C and 5kb. Am J Sci 281:1249–1516.

Hemingway BS, Robie RA. 1984. Thermodynamic properties of zeolites: Low-temperature heat capacities and thermodynamic functions for phillipsite and clinoptilolite. Estimates of the thermochemical properties of zeolitic water at low temperature. Am Mineral 69:692–700.

Holland TJB. 1989. Dependence of entropy on volume for silicate and oxide minerals: A review and a predictive model. Am Mineral 74:5–13.

Honda A, Muffler LJP. 1970. Hydrothermal alteration in core from research drill hole Y-1, Upper Geyser Basin, Yellowstone National Park, Wyoming. Am Mineral 55:1714–1737.

Howell DA, Johnson GK, Tasker IR, O'Hare PAG, Wise WS. 1990. Thermodynamic properties of the zeolite stilbite. Zeolites 10:525–531.

Iijima A. 1975. Effect of pore water to clinoptilolite-analcime-albite reaction series. J Fac Sci, Univ Tokyo, Sec II 19:133–147.

Iijima A. 1978. Geologic occurrences of zeolites in marine environments. In: Sand LB, Mumpton FA, editors. Natural zeolites: Occurrence, properties, use. New York: Pergamon Pr. p 175–198.

Johnson GK, Flotow HE, O'Hare PAG, Wise WS. 1982. Thermodynamic studies of zeolites: Analcime and dehydrated analcime. Am Mineral 67:736–748.

Johnson GK, Flotow HE, O'Hare PAG, Wise WS. 1985. Thermodynamic studies of zeolites: Heulandite. Am Mineral 70:1065–1071.

Johnson GK, Tasker IR, Jurgens R, O'Hare PAG. 1991. Thermodynamic studies of zeolites: Clinoptilolite. J Chem Thermodynamics 23:475–484.

Johnson GK, Tasker IR, Flotow HE, O'Hare PAG, Wise WS. 1992. Thermodynamic studies of mordenite, dehydrated mordenite, and gibbsite. Am Mineral 77:85–93.

Johnson JW, Oelkers EH, Helgeson HC. 1991. SUPCRT92: A software package for calculating the standard molal thermodynamic properties of minerals, gases, aqueous species, and reaction from 1 to 5000 bars and 0° to 1000°C: Earth Sciences Dept, L-219, Lawrence Livermore National Laboratory, Livermore, CA. 80 p.

Johnstone JK, Peters RR, Gnirk PF. 1984. Unit evaluation at Yucca Mountain, Nevada Test Site: Summary report and recommendations. Sandia National Laboratory Report SAND83-0372.

Jones BF, Rettig SL, Eugster HP. 1967. Silica in alkaline brines. Science 158:1310–1314.

Keith TEC, White DE, Beeson MH. 1978. Hydrothermal alteration and self-sealing in Y-7 and Y-8 in northern part of Upper Geyser Basin, Yellowstone National Park, Wyoming. USGS Prof Paper 1054-A. 26 p.

Kerrisk JF. 1983. Reaction-path calculations of groundwater chemistry and mineral formation at Rainier Mesa, Nevada. Los Alamos National Laboratory Report LA-9912-MS. 41 p.

Kerrisk JF. 1987. Groundwater chemistry at Yucca Mountain, Nevada, and vicinity. Los Alamos National Laboratory Report LA-10929-MS. 118 p.

Knauss KG, Beiriger WJ, Peifer DW. 1985. Hydrothermal interaction of crushed Topopah Spring Tuff and J-13 water at 90, 150, and 250°C using Dickson-type, gold-bag rocking autoclaves. Lawrence Livermore National Laboratory Report UCRL-53630. 27 p.

Knauss KG, Beiriger WJ, Peifer DW. 1987. Hydrothermal interaction of solid wafers of Topopah Spring Tuff with J-13 water at 90 and 150°C using Dickson-type, gold-bag rocking autoclaves: Long-term experiments. Lawrence Livermore National Laboratory Report UCRL-53722. 21 p.

Knauss KG, Beiriger WJ, Peifer DW, Piwinskii AJ. 1985. Hydrothermal interaction of solid wafers of Topopah Spring Tuff with J-13 and distilled water at 90, 150, and 250°C, using Dickson-type, gold-bag rocking autoclaves. Lawrence Livermore National Laboratory Report UCRL-53645. 55 p.

Knauss KG, Peifer DW. 1986. Reaction of vitric Topopah Spring Tuff and J-13 ground water under hydrothermal conditions using Dickson-type, gold-bag rocking autoclaves. Lawrence Livermore National Laboratory Report UCRL-53795. 39 p.

Mumpton FA. 1960. Clinoptilolite redefined. Am Mineral 45:351–369.

Murphy WM. 1994. Geochemical models for gas-water-rock interactions in a proposed nuclear waste repository at Yucca Mountain, Nevada. Proc Site Characterization and Model Validation Focus '93: American Nuclear Society. p 115–121.

Murphy WM, Pabalan RT. 1994. Geochemical investigations related to the Yucca Mountain environment and potential nuclear waste repository. US Nuclear Regulatory Commission Report NUREG/CR-6288. 190 p.

Pabalan RT, Bertetti FP. 1994. Thermodynamics of ion-exchange between Na$^+$/Sr^{2+} solutions and the zeolite mineral clinoptilolite. Mat Res Soc Symp Proc 333:731–738.

Pabalan RT, Murphy WM. 1990. Progress in experimental studies on the thermodynamic and ion exchange properties of clinoptilolite. Center for Nuclear Waste Regulatory Analyses, CNWRA 89-006, San Antonio, TX. 39 p.

Perry E, Hower J. 1970. Burial diagenesis in Gulf Coast pelitic sediments. Clays Clay Miner 18:165–177.

Perfect DL, Faunt CC, Steinkampf WC, Turner AK. 1995. Hydrochemical data base for the Death Valley Region, California and Nevada. USGS Open File Report 94–305. 10 p.

Robinson GR Jr, Haas JL Jr. 1983. Heat capacity, relative enthalpy, and calorimetric entropy of silicate minerals: An empirical method of prediction. Am Mineral 68:541–553.

Sheppard RA, Gude AJ 3rd. 1968. Distribution and genesis of authigenic silicate minerals in tuffs of Pleistocene Lake Tecopa, Inyo County, California. USGS Prof Pap 597. 38 p.

Sheppard RA, Gude AJ 3rd. 1969. Diagenesis of tuffs in the Barstow Formation, Mud Hills, San Bernardino County, California. USGS Prof Pap 634. 35 p.

Sheppard RA, Gude AJ 3rd. 1973. Zeolites and associated authigenic silicate minerals in tuffaceous rocks of the Big Sandy Formation, Mohave County, Arizona. USGS Prof Pap 830. 36 p.

Smyth JR. 1982. Zeolite stability constraints on radioactive waste isolation in zeolite-bearing volcanic rocks. J Geol 90:195–202.

Smyth JR, Caporuscio FA. 1981. Review of the thermal stability and cation exchange properties of the zeolite minerals clinoptilolite, mordenite, and analcime: Applications to radioactive waste isolation in silicic tuff. Los Alamos National Laboratory Report LA-8841-MS. 30 p.

Surdam RC, Sheppard RA. 1978. Zeolites in saline, alkaline-lake deposits. In: Sand LB, Mumpton FA, editors. Natural zeolites: Occurrence, properties, use. New York: Pergamon Pr. p 145–174.

Vaughan DEW. 1978. Properties of natural zeolites. In: Sand LB, Mumpton FA, editors. Natural zeolites: Occurrence, properties, use. New York: Pergamon Pr. p 353–371.

White AF, Claassen HC, Benson LV. 1980. The effect of dissolution of volcanic glass on the water chemistry in a tuffaceous aquifer, Rainier Mesa, Nevada. USGS Geol Survey Water-Supply Pap 1535-Q. 34 p.

Wilkin RT, Barnes HL. 1995. Solubilities of the zeolites analcime and Na-clinoptilolite in hydrothermal solutions. In: Barnes HL, editor. V. M. Goldschmidt Conf, Program and Abstracts. 97 p.

Yang IC. 1992. Flow and transport through unsaturated rock—data from two test holes, Yucca Mountain, Nevada. Proc 3rd Annu High Level Radioactive Waste Management Meeting; Las Vegas, NV. p 732–737.